

## Torque Improvement in a Buried-Type IPM Bearingless Motor With a Novel Rotor Structure

**Masashi Sakagami, Akira Chiba**

Department of Electrical Engineering, Faculty of Science and Technology  
Tokyo University of Science, 2641 Yamazaki, Noda, Chiba, Japan  
chiba@ee.noda.tus.ac.jp

**Masahide Ooshima**

Department of Electronic Systems Engineering, Faculty of Systems Engineering  
Tokyo University of Science, Suwa, 5000-1 Toyohira Chino Nagano Japan

**Tadashi Fukao**

Department of Electrical Engineering, Faculty of Technology  
Musashi Institute of Technology, Tamazutsumi, Setagaya-ku, Tokyo, Japan

### ABSTRACT

In this paper, torque improvement in rotor designs of permanent magnet bearingless motors is described. Novel rotor structures are proposed with modification of buried permanent magnet rotors. The torque and suspension force are obtained through Finite Element Analysis (FEM). It is shown that the torque is enhanced 80% while the suspension force is competitive.

### INTRODUCTION

Recently, bearingless motors have been developed and actively researched in the world. The bearingless motors are hybrids of electric motors and magnetic bearings. They have some advantages such as small size and light weight as well as low cost. The bearingless motors have some possible applications of semiconductor process, information storage drives, compressors, liquid pumps, blood pumps, and etc. The principle of bearingless motors can be applied to some kinds of conventional motor types, for example, induction [1], surface mounted PM [2-4], inset PM [5], consequent-pole PM [6], buried and interior PM [7-9], homopolar hybrid [10-11], synchronous reluctance and switched reluctance types [12-13].

In recent years, the efficiency has been improved in motor drives thanks to extensive developments of PM motors by manufacturers to save global environments reducing the CO<sub>2</sub> emission. Interior Permanent Magnet (IPM) synchronous motors are becoming most used in wide spread industrial applications. The IPM motors expand a speed range of constant output operation and adjustable speed area by using field-weakening control. In addition, the reluctance torque as well as the PM torque is also generated. The rotor design is rather free in the PM shape

and size as well as the iron pole structure. Rare earth permanent magnets are buried in rotor silicon steel lamination. In the bearingless PM motors, the conventional IPM rotors are not very suitable in a point of view of efficient torque generation.

In this paper, a novel rotor structure is proposed for the buried-type IPM (BPM) bearingless motors. The torque improvement for given stator current is described.

### STRUCTURE OF BPM ROTOR WITH SALIENT-POLES

Fig.1 shows the rotor cross section of the proposed BPM bearingless motor by authors previously [7-8] (Hereafter, it is referenced as rotorA). To enhance suspension force at no torque load, thin PMs are designed. To avoid irreversible demagnetization, iron bridges

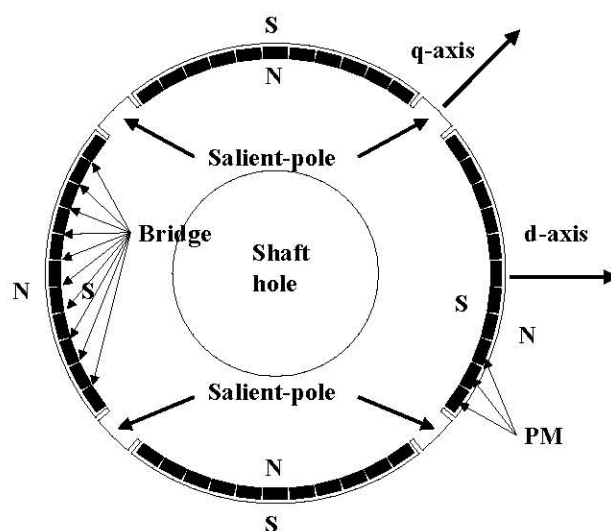


Fig.1 Rotor cross section of the proposed BPM bearingless motor previously (Rotor A)

are constructed between PMs. In the bridges, leakage fluxes are generated, and the irreversible demagnetization is prevented up to a certain current condition. This rotor needs no guard ring because the PMs are buried. Therefore, the airgap length between the rotor and the stator can be small. The suspension force for unity current is larger than those of surface and inset PM types. And the PMs are protected against the centrifugal force in high speed operation. The salient-poles between magnetic poles contribute to enlarge the armature reaction flux, so that the suspension force is enhanced at torque generation.

**ROTOR STRUCTURE TO PREVENT LEAKAGE FLUX**

The rotor in Fig.1 has excellent capability for suspension force generation for the given suspension MMF. However, the torque generation is not enough because the leakage fluxes in the bridges result in a decrease in main flux. In FEM analysis, the torque is enhanced 1.6 times if the iron bridges are removed and filled with the PMs. However, such thin circular shaped PM is not easy to fabricate. In addition, both ends of magnetic poles are sensitive to irreversible demagnetization. Thus, to prevent irreversible demagnetization, PMs in both ends of magnetic poles should be thick.

Fig.2 shows a cross section of the proposed rotor having thick PMs at the ends of magnetic poles (rotor B). The leakage fluxes are not generated significantly because the bridges were removed. Therefore, the MMF generated from PMs can be effectively used. The suspension

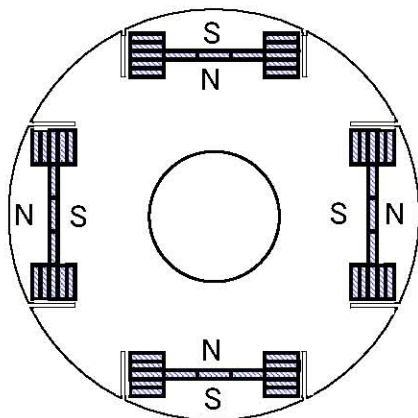


Fig.2 Cross section of proposed IPM rotor (Rotor B)

force does not decrease at no torque current because the center part PMs are thin. The circular arc shaped PM is not used, thus production is rather easy with rectangular PMs with the same shape.

**ANALYTICAL RESULT OF TORQUE**

Fig.3 shows analytical FEM results of the torque of rotor B with respect to the current phase angle. The motor current is changed from 2A to 10A while the suspension force current is kept at a constant value. The rotor angular position is varied from 0° to 30° at an interval of 3°, and the average torque is plotted for each motor current condition. In the analysis, the rotor outer diameter, the airgap length and stack length are 49.2mm, 0.4mm and 50mm, which are the same as those of rotorA, respectively. When the field weakening control is adapted, the proposed rotor torque is about 1.5Nm, i.e. 50% higher than rotor A at the rated current of 8A. The torque enhancement is realized because the leakage flux in the bridges is less, and the reluctance torque is increased due to the better salient ratio. The optimum field weakening current angle  $\beta$  is described by the dotted curve.

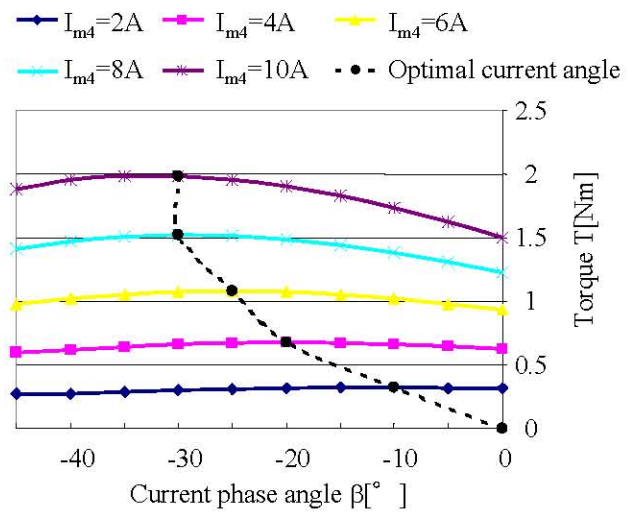


Fig.3 Torque analysis of rotor B

**ANALYTICAL RESULT OF SUSPENSION FORCE**

Fig.4 shows analytical results of the suspension force of rotor B with respect to the current phase angle. The analytical condition is similar to the previous torque analysis. At  $\beta=0^\circ$ , the suspension force is increased as the

motor current is increased up to 6A, but it is decreased by magnetic saturation more than the current of 6A. The decrease in suspension force can be prevented by adjusting the current phase angle, i.e., adapting the field weakening control. The dotted line indicates the maximum suspension force trajectory. The trajectory indicates that the current phase angle should be led for the better suspension force as the motor current is increased.

From the analyzed results in Figs. 3 and 4, one can see that the phase lead in the motor winding current results in both the better torque and suspension force. However, the optimal trajectories are not the same. Fig.5 compares two trajectories. In addition, the trajectories are also drawn for 5% reduction in suspension force generation in Fig.5. Note that the suspension force reduction is within 5% under the rated current even though the optimal torque trajectory is selected. Thus, the optimal torque trajectory should be chosen.

Fig.6 compares the suspension forces of rotors A and B. It is seen that the better suspension force is generated in rotor B.

**FURTHER IMPROVEMENT TO ENHANCE TORQUE GENERATION**

Rotor B has better torque performance compared with rotor A. The main factor is due to the reduced leakage fluxes around PMs and the enlarged salient-poles. In the similar idea, further torque improvement is possible by rotor structure design optimization. In rotor B design, PM thickness and width have been optimized considering practical PM and silicon steel fabrication. Rotor B is one of optimized structures. Let us see if there is a room for improvement.

Fig.7 shows flux lines around a magnetic pole. Both the suspension and torque currents are supplied at the rated value. If the fluxes can be gathered in teeth a, b and c, the torque is improved. This basic idea is achieved by inserting PMs at both ends of the magnetic pole. Fig.8 shows the proposed novel BPM rotor structure (rotor C). Two PMs are added at the positions where slits are constructed. These PMs contribute to magnetically saturate leakage flux paths at the end of magnetic poles.

Fig.9 shows flux lines of the novel rotor around a magnetic pole. The magnetic fluxes of three stator teeth a, b and c are increased about 10% depending on teeth positions

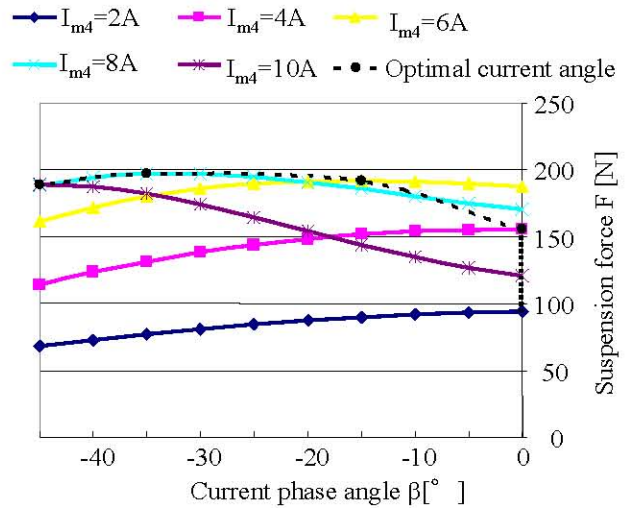


Fig.4 Suspension force analysis of rotor B

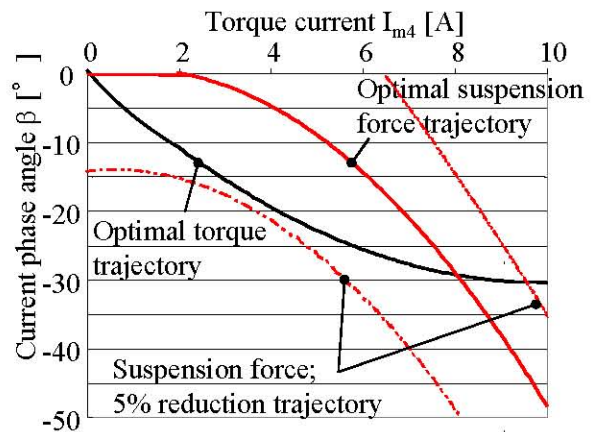


Fig.5 Comparison of optimal trajectories

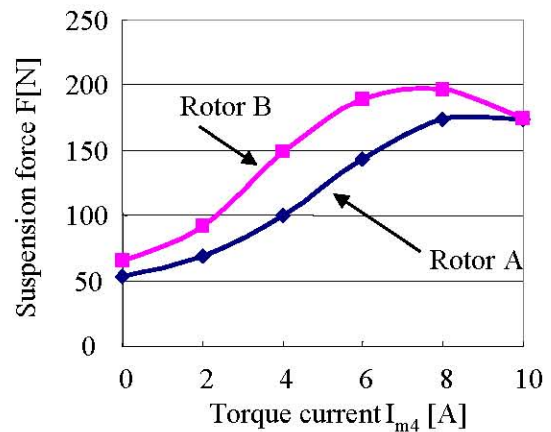


Fig.6 Comparison of suspension forces



compared with those in rotor B described in Fig.7.

Fig.10 confirms that the torque is enhanced in rotor C compared with rotors A and B. The torque is analyzed with a variation of phase angle from  $-45$  to  $0^\circ$  at an interval of  $5^\circ$ . The current condition is the same as that in Fig.3. The dotted line is a trajectory maximizing torque for given motor current. The maximum torque is  $1.82\text{Nm}$  of  $I_{m4}=8\text{A}$ , which is about 1.8 times of that in rotor A. It is about 1.2 times of that in rotor B.

Fig.11 shows results of suspension force analysis of rotor C. A unique point of rotor C is that magnetic saturation starts at low current compared with rotor B. The suspension force decreases to  $90\text{N}$  when the motor current is  $10\text{A}$  at  $\beta=0^\circ$ , however the previous rotor B has decreased up to  $120\text{N}$  at  $10\text{A}$ . Even if the field weakening control is introduced, rotor C generates less magnetic suspension force by about  $20\text{N}$  in comparison to rotor B. However, it is

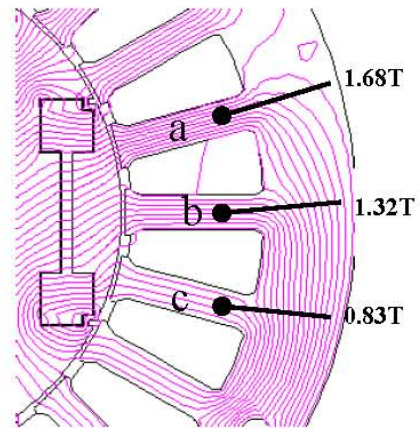


Fig.9 Flux line chart of rotor C

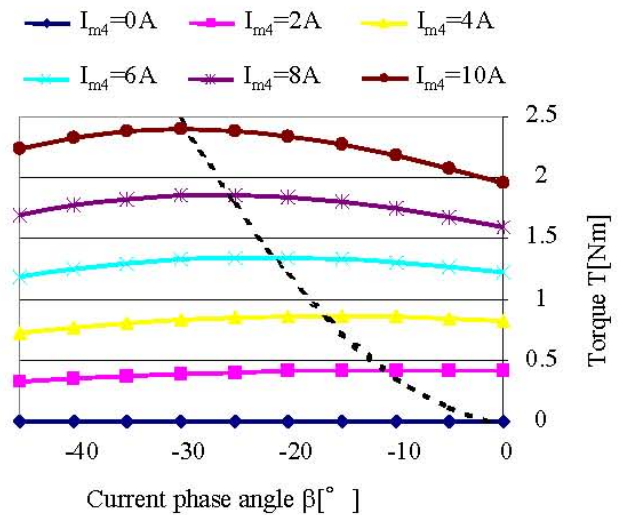


Fig.10 Torque analysis of rotor C

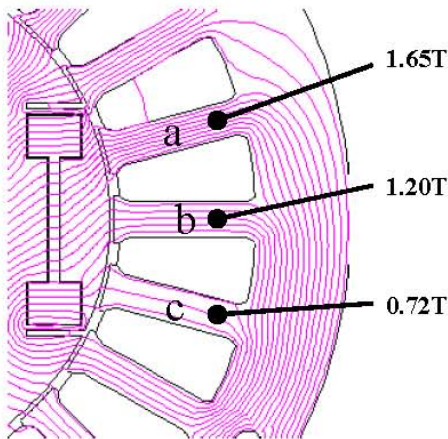


Fig.7 Flux line chart of rotor B

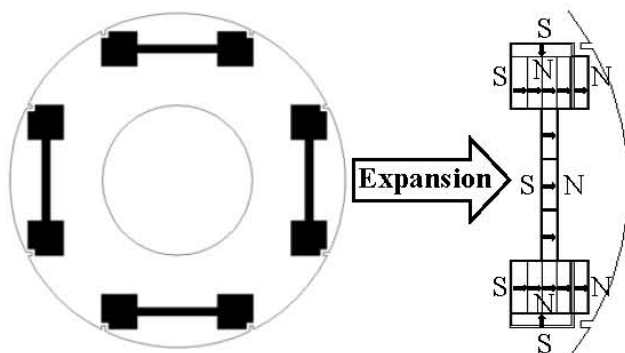


Fig.8 Novel BPM rotor structure (Rotor C)

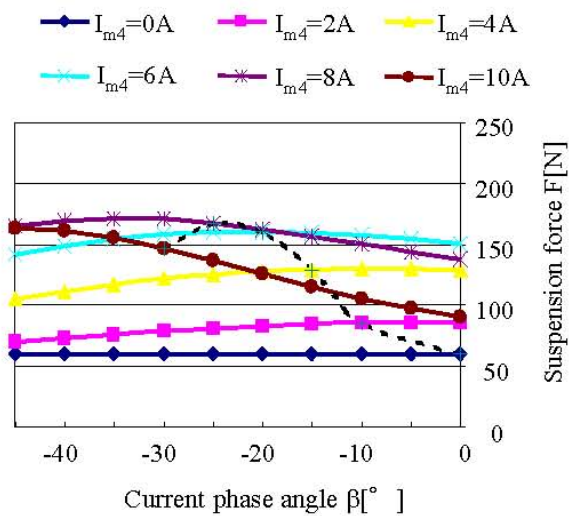


Fig.11 Suspension force analysis of rotor C

competitive to rotor A. The reason is that magnetic saturation occurred in the stator teeth because the flux density is enhanced in rotor C.

Fig.12 compares the torques of rotors A and C. The field weakening control is applied for rotor C to maximize the torque. The torque per unity current of rotor C is 0.23Nm/A, which is about 1.7 times of that in rotor A.

In Fig.13 the suspension forces are compared between rotors A and C. The suspension force is mostly competitive. An increase in torque with competitive suspension force is achieved.

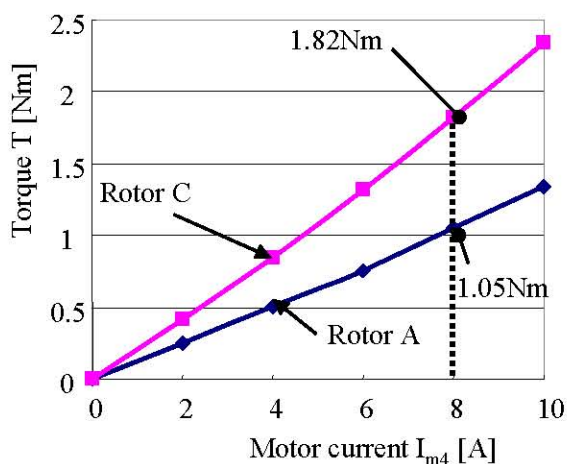


Fig.12 Torque comparison of rotors A and C

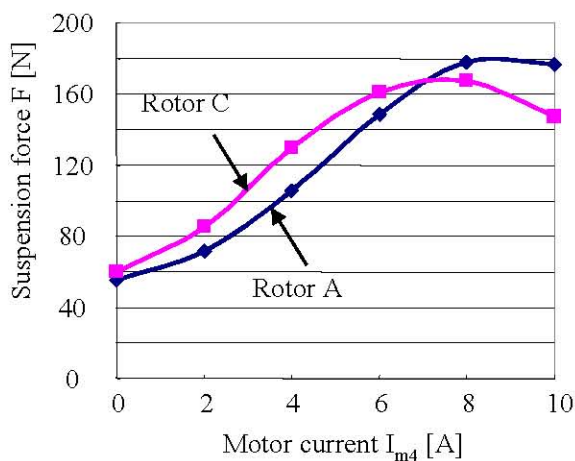


Fig.13 Comparison of suspension force of rotors A and C

## CONCLUSION

In this paper, a novel rotor structure for the BPM bearingless motors is proposed. The torque is enhanced with competitive suspension force for a given stator winding MMF. In FEM analysis, the torque is increased to 1.82Nm at rated point, which is 1.8 times of the original rotor.

## ACKNOWLEDGMENT

The authors would like to thank Mr. Takeshi Kurokawa who was a graduate student at the Tokyo University of Science.

## REFERENCE

- [1] Akira Chiba, Tadashi Fukao, "Optimal design of rotor circuits in induction type bearingless motors", IEEE Trans On Mag, Vol.34, No.4, pp.2108-2110, Jul.1998
- [2] Masahide Ooshima, Satoru Miyazawa, Akira Chiba, Fukuzo Nakamura, Tadashi Fukao, "Performance Evaluation and Test Results of a 11,000r/m, 4kW Surface-Mounted Permanent Magnet-Type Bearingless Motor", ISMB, ETH Zurich pp.377-382, August 23-25, 2000
- [3] Barret Steele, Lyndon Stephens, "A Test Rig for Measuring Force and Torque Production in a Lorenz, Slotless Self Bearing Motor", ISMB, ETH Zurich pp.407-412, August 23-25, 2000
- [4] Klaus Nenninger, Wolfgang Amrhein, Siegfried Silber, "Bearingless Single-phase Motor with Fractional Pitch Windings" ISMB, ETH Zurich pp.371-375, August 23-25, 2000
- [5] Kohei Inagaki, Akira Chiba, M.A.Rahman, Tadashi Fukao, "Performance Characteristics of Inset-Type Permanent Magnet Bearingless Motor Drives", PESWM, 23-27 January 2000 Singapore
- [6] Tomohiro Takenaga, Yutaka Kubota, Akira Chiba, Tadashi Fukao "A Principle And Winding Design of Consequent-Pole Bearingless Motors" JSME International Journal Series C vol.46, no.2. pp. 363-369 June 2003
- [7] Masahide Ooshima, Satoru Miyazawa, Yusuke Shima, Akira Chiba, Fukuzo Nakamura, Tadashi Fukao, "Increase in Radial Force of A Bearingless Motor with Buried Permanent Magnet-Type Rotor", Proceedings of the Fourth International conference on MOVIC, vol.3, pp. 1077-1082,1998

- [8] Noriaki Fujie, Rintarou Yoshimatsu, Akira Chiba, Masahide Ooshima, M.A.Rahman, and Tadashi Fukao, "A Decoupling control Method of Buried Permanent Magnet Bearingless Motors considering Magnetic Saturation", IPEC-Tokyo 2000, S-10-6 pp. 395-400 2000
- [9] Masatsugu Takemoto, Michio Uyama, Akira Chiba, Hirofumi Akagi, Tadashi Fukao, "A Deeply-Buried Permanent Magnet Bearingless Motor with 2-pole Motor Windings and 4-pole Suspension Windings" IEEE IAS Annual Meeting Conference Record, Salt Lake City pp.1413-1420 2003 Oct.
- [10] Osamu Ichikawa, Akira Chiba, Tadashi Fukao, "Principles and Structure of Homopolar Type Bearingless Motors", IPEC-Tokyo pp.401-406 2000
- [11] Seung-Jong Kim, Tatsunori Shimonishi, Hideki Kaneboko, Yohji Okada, "Design of a Hybrid-Type Short-Span Self-Bearing Motor" ISMB, Eth Zurich pp.359-364, August 23-25, 2000
- [12] Osamu Ichikawa, Chikara Michioka, Akira Chiba, Tadashi Fukao, "An Analysis of Radial Forces and Rotor Position Control Method of Reluctance Type Bearingless Motors" The Transactions of The Institute of Electrical Engineers of Japan - D, vol.117 pp.1123-1131 1997
- [13] Masatsugu Takehiro, Akira Chiba, Hirofumi Akagi, Tadashi Fukao, "Radial Force and Torque of a Bearingless Switched Reluctance Motor Operating in a Region of Magnetic Saturation" IEEE Transaction on Industry Applications, vol. 40, no.1, pp.103-112 January/February 2004